REFERENCE : TE 04

TITLE : DETERMINATION OF ISOLATED ROTOR TRANSFER FUNCTIONS
IN THE ONERA S1.MA WIND TUNNEL

AUTHORS :
P. CROZIER / ONERA GMT / DTEX
P. EGLIN / EUROCOPTER Marignane
A. DESOPPER / ONERA DCSD Salon

Brite Euram project BE-95-1311 HELIFLOW includes investigations into specific problems of helicopter flight mechanics. Task no. 6 of that project is dedicated to the measurement of isolated helicopter rotor dynamic transfer functions for different configurations (advance ratio, lift). Such tests were performed in ONERA S1.MA wind tunnel in December 1997.

This document recalls the general purpose of the test, presents the test means, the test methodology and finally a sample of results.

This work was supported by the EUROPEAN UNION under the Brite Euram programme.

1. TEST OBJECTIVES

Task 6 of Brite Euram HELIFLOW project is dedicated to the measurement of isolated helicopter rotor dynamic transfer functions. Such measurements have been performed in ONERA S1.MA wind tunnel.

For these tests a Mach scaled four bladed rotor of 4.2 meters in diameter has been used and sinusoidal inputs were introduced successively on collective, lateral and longitudinal pitch angles. The excitations were realised with a maximum amplitude of 1° and frequencies between 0.5 and a maximum of 22 Hz so well over the rotation frequency set at 16 Hz.

The transfer functions of the balance forces and moments non corrected and corrected from inertia, of the blade pitch, flap and lead-lag angles have been obtained for 5 advance ratios (μ = 0, 0.15, 0.3, 0.37, 0.42) at a normal lift force of Ct/sigma=0.075 and for 2 lift forces (Ct/sigma=0.075 and 0.1) at an advance ratio of 0.37.

The main objective of these tests is to obtain a transfer functions data base for an isolated rotor in a frequency range interesting for handling qualities studies. In particular this will allow to look at the off axis responses and to validate and improve flight mechanic codes.

2. WIND TUNNEL TESTS

2.1 Test rig

The rig has been designed to test helicopter rotor and tilt rotor with diameters up to 5 meters and to be installed in one of the three movable test sections of the large S1MA wind tunnel of the ONERA Modane-Avrieux Centre (Ref. 1). The test section is 8 meters in diameter and 14 meters in length. This wind tunnel can reach Mach number 1 but for helicopter rotor tests the maximum airspeed is 130 m/s.

The main features of this rig are :
- rotation in clockwise or counter clockwise direction ;
- rotation speed between 0 and 1100 rpm;
- accurate stability of the rotation speed even with a parameter variation ;
- maximum power 500 kW ;

- maximum torque 7000 mN at 680 rpm ;
- tilt angle range +20° to -95° with a positioning accuracy of ±0.02 degrees ;
- maximum tilting rate 2° per second.

The test rig also includes a slipring located inside the drive shaft. It transmits the sensor signals from the rotating to the fixed parts. It includes 137 measurement tracks and 13 power tracks.

To perform HELIFLOW test (dynamic excitations up to 22 Hz) it was necessary to change the whole hydraulic system of the test rig. For classical static helicopter rotor tests, hydraulic flow does not exceed 7 l/min. For HELIFLOW dynamic tests it was necessary to reach a 20 l/min flow with a pressure loss as small as possible. From the hydraulic compressor to the actuators, the tubes pass through the test cart, the test rig and especially from the fixed part to the tilting part of the test rig. Until now the pressure loss was around 10 bar with a flow of 7 l/min but would have reached 60 bar for Heliflow tests. Such a situation was not acceptable.

ONERA decided therefore to improve this circuit as far as possible considering the small space available, especially in the test rig. With the new circuit, the pressure loss, with a flow of 20 l/min, is decreased to 5.7 bar.

2.2 Test rig instrumentation

The instrumentation of the test rig includes a balance, a torquemeter, flectors and eight accelerometers.

The balance is a non-rotating balance with assembled plates, connected by six dynamometers (capacity 20000N). Three dynamometers measure the lift force, the roll and the pitch moments, two measure the lateral force and the friction moment of the hub and the other one measures the propulsive force. The balance is also equipped with a safety device which can lock the upper plate if one of the dynamometers exceeds a pre-set load or in case of trouble with the hydraulic piloting system of the hub.

The torquemeter is a thin tube used to measure the motor torque supplied to the hub. It is located on the transmission line inside the balance and has a capacity of 3 000 Nm.

The flectors which are an elastic decoupling device, are located on both sides of the torquemeter. They transmit the motor torque but are very flexible in other planes so as not to short-circuit the balance. The residual lift force due to the flectors is measured by a strain gage located on the upper flector. Thanks to the balance, torquemeter and flectors an accuracy in rotor performance measurements of approximately ±1% is obtained.

Furthermore, eight accelerometers positioned on the fixed part of the hub are used to determine the inertial forces. These forces are combined with the raw forces measured by the balance to obtain the dynamic forces and moments at hub centre.

2.3 Rotor hub

This hub is a four bladed one, articulated in flap, pitch and lead-lag. The lead-lag and flapping hinges are at the same location 0.075 m from the hub centre. The pitch hinge is located beyond these hinges. Angular frequency adaptors are installed on the lead-lag hinge.

The swash-plate is actuated by three hydraulic actuators located at 120 degrees positions. The servo-system have high mass flow in order to achieve frequencies up to 22 Hz .The collective and cyclic pitch angles can be controlled from the test room.

The hub is equipped with different sensors :
- strain gages for monitoring the stress on each pitch rod and on the rotating and fixed scissors ;
- mast bending moments are measured at four different locations ;
- pitch, flap and lead-lag angles are measured on each blade ;
- six accelerometers are fixed on the rotating part of the hub ;
- three displacement sensors measure the actuator strokes. Their signals are used to pilot the controls.

2.4 Rotor blades

The blade technology is very close to the one used for full scale composite rotor blades. The spar is made of glass-fibber roving and the rear part is filled with honeycomb. The skin consists of layers of carbon-fibber at 45 degrees. The chord-wise balancing is achieved through adding Inermet counterweight embedded into the spar.

From a dynamic point of view, these blades are not identical to those of a full scale rotor : the first flapping and drag modes are positioned as on a full scale rotor, but the frequency of the first torsion mode is higher than that encountered on most EUROCOPTER helicopter.

The main characteristics are :
- reference chord : 0.1593 m
- rotor radius : 2.1 m
- solidity : 0.0966

Chord distribution :

Position	0.2 R to 0.92 R	1.0 R
Chord (m)	0.168	0.056

Blade twist :

Position	0.2 R	0.85 R	0.92 R	1.0 R
(°)	5.4	-2.37	-2.488	-3.448

Airfoil distribution :

Position	0.2 R to 0.85 R	0.92 R to 1.0 R
Airfoil	OA312	OA309

Gages located at different radius can be used to determine the flapping, drag and torsion moments along the blades. Only some of them were measured for blade monitoring reasons.

3. TEST METHODOLOGY

3.1 Balance dynamic calibration

In order to obtain the transfer functions of the balance corrected from inertia effects, a dynamic calibration was performed without rotation. The inertia correction is obtained with the measurements of the eight accelerometers located on the fixed part of the hub. An electro-dynamic shaker was used to apply a well known sinusoidal force to the hub (Fex). In X direction, for example, the force measured by the balance is XB and the final force, after inertia correction is XA. The transfer functions computed are the transfer function of XB over Fex and XA over Fex. The method is satisfactory when the transfer function XA/Fex has a gain of one and a phase equal to zero on the axis on which the shaker is acting.

The general dynamic equations are as follow :

$$XA = XB + M * \ddot{X}_G$$

$$YA = YB + M * \ddot{Y}_G$$

$$ZA = ZB + M * \ddot{Z}_G$$

$$LA = LB + A_G * \dot{p} + Cm * q * 2 * \pi * F$$

$$-M * z_G * \ddot{Y}_G + M * y_G * \ddot{Z}_G$$

$$MA = MB + B_G * \dot{q} - Cm * q * 2 * \pi * F$$

$$+ M * z_G * \ddot{X}_G - M * x_G * \ddot{Z}_G$$

with :
- XB, YB, ZB, LB and MB raw forces measured by the balance ;

- M mass of the weighed part of the hub ;

- $\left(x_G, y_G, z_G \right)$ location of the mass centre G ;

- $\left(\ddot{X}_G, \ddot{Y}_G, \ddot{Z}_G \right)$ linear acceleration at mass centre;

- $\left(\dot{p}, \dot{q}, \dot{r} \right)$ rotating acceleration at mass centre ;

- $\begin{pmatrix} A_G & 0 & 0 \\ 0 & B_G & 0 \\ 0 & 0 & C_G \end{pmatrix}$ inertia matrix of weighed part of the hub (at mass centre)

- $\begin{pmatrix} A_m & 0 & 0 \\ 0 & B_m & 0 \\ 0 & 0 & C_m \end{pmatrix}$ inertia matrix of rotating part of the hub

- XA, YA, ZA, LA and MA corrected forces and moments at rotor hub centre.

During the balance calibration, the hub is not rotating so F = 0 in the previous formula.

Figures 1a to 1d present the transfer functions obtained in X direction for raw and corrected balance forces.
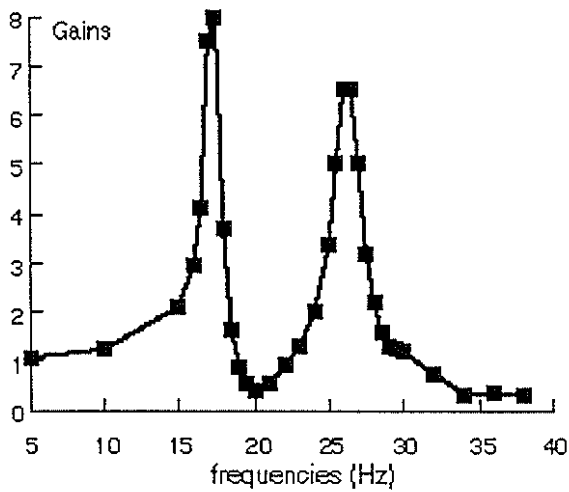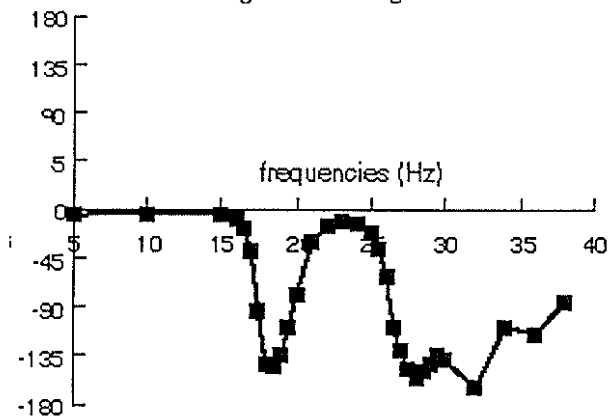
Figure 1a : XB gains
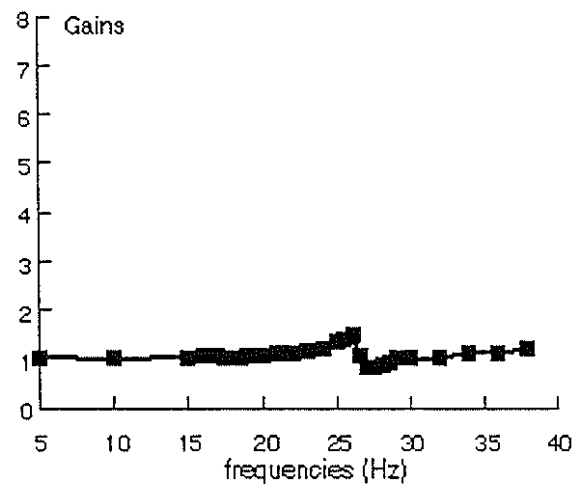

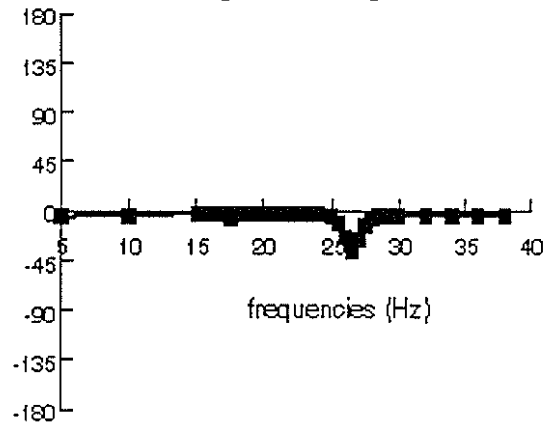**Figure 1b : XB phases (degrees)**

Figure 1c : XA gains

Figure 1d : XA phases (degrees)

One can see great changes in gain and phase for raw force transfer function. However when inertia corrections are introduced, the final gains are about 1 and the phases about zero for the frequencies we are interested in. This validates the dynamic calibration of the balance. The same results are obtained for the other forces and moments.

3.2 Rotor static control

For the static conditions, the following parameters :

- advancing Mach number (M0);
- rotor rotational speed (RPM);
- rotor shaft tilt angle (α);
- collective pitch (T0V);
- cyclic pitch angles (TC1V, TS1V), were adjusted to match the six conditions :

- advance ratio (μ);
- rotational frequency (F);
- lift coefficient (Ct/sigma);
- propulsive coefficient ((CxS)f/Ssigma);
- zero first harmonic flapping.

Once the static conditions were reached a special control system was activated to perform the dynamic piloting inputs.

3.3 Rotor dynamic control

In order to estimate the dynamic transfer functions a sinusoidal input was introduced successively on each control axis. The requested frequencies were i * F / 32 with i between 1 and 44 so frequencies from 0.5 Hz to 22 Hz with an amplitude ranging from 0.5° to 1°. The maximum frequency 22 Hz was clearly over the rotation frequency (F=16 Hz).

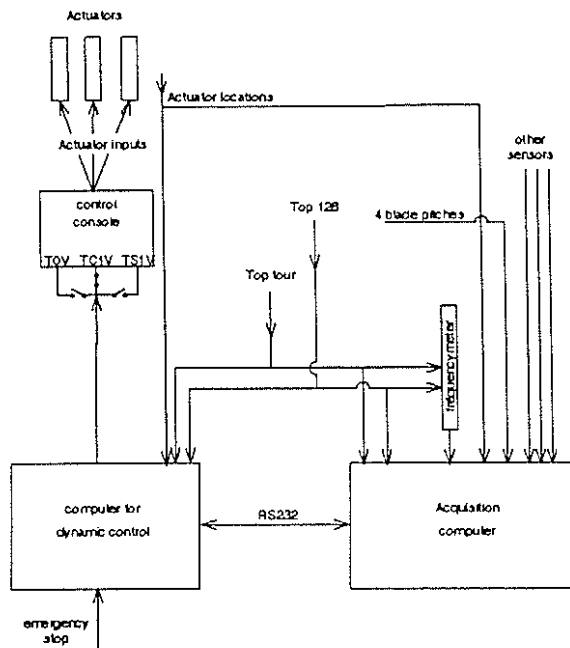The control system was prepared by EUROCOPTER and ONERA. Its block diagram is shown in figure 2.

Figure 2 : control system block diagram

The main parts of this system are the control console, the computer for dynamic control inputs and the acquisition computer.

The control console and dynamic controls computer are described below and the data acquisition in 3.5.

A specific console is used for all the helicopter tests in S1MA, it ensures the control of the three actuators of the swash plate. On its front face three potentiometers are used to set the static collective and cyclic pitch angles. On its rear face three plugs, one per pitch angle, can be used to introduce dynamic inputs.

The aim of the dynamic controls computer is to generate a sinusoidal signal at desired amplitude and frequency to be introduced on the control console. To automatically generate the required frequency, the computer has an input of two signals, called top tour and top 128 respectively. The first one gives the hub rotation frequency and the second one can be considered as the "hub clock" with a rate of 128 points per revolution. To achieve the right amplitude there is a loop system. The computer has the actuator location signals as input, and thanks to these signals the dynamic pitch angles are calculated

in real time and printed on the computer screen. Using a potentiometer, the rotor pilot can adjust the amplitude of the dynamic signal. For safety purpose, the excitation generation could always be stopped by the rotor pilot.

When the system was tested for the first time, the different excitations were coupled. For example, figure 3 shows a quite large coupling in collective (T0V) and longitudinal (TS1V) for dynamic inputs in lateral (TC1V).
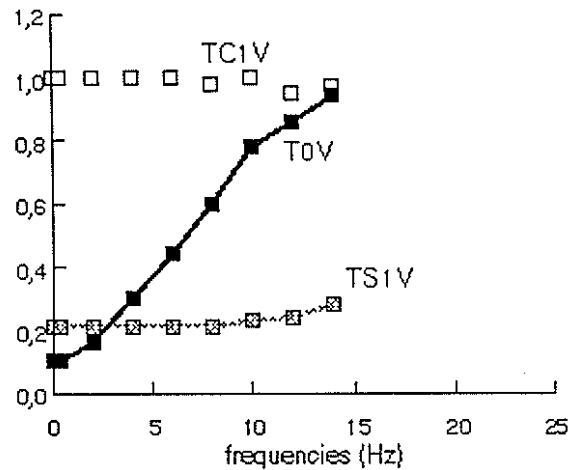

Figure 3 : coupling before optimisation

These problems were solved with a detailed study of the control system behaviour with dynamic inputs and an accurate adjustment was found for the whole excitation range.

Figure 4 shows the results for lateral excitations after the control system optimisation.
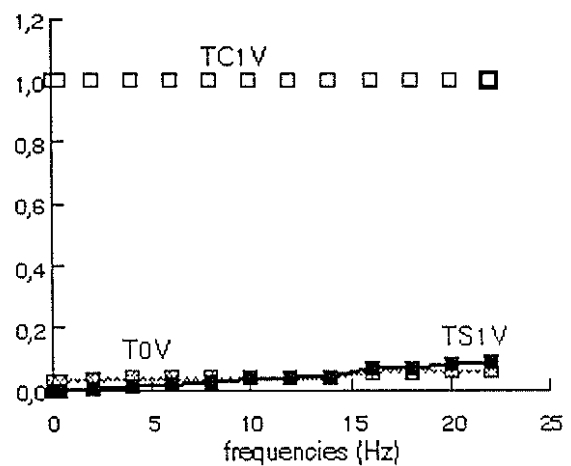

Figure 4 : coupling after optimisation

The remaining couplings are quite small. The same results were obtained for collective and longitudinal pitch angle excitations.

3.4 Test procedure

The following procedure was adopted for the tests :
- Wind-off measurements without blade : all the frequencies requested were successively realised. From this, the inertia influence of the actuator motions was obtained.
- Wind-on tests with the blades : when the requested steady conditions were reached, a point without excitation was acquired as dynamic zero and then, all the frequencies requested were realised.

3.5 Data acquisition

To improve the productivity of the tests, an automatic dialogue between the computer for dynamic control and the acquisition system has been implemented (figure 2).

This dialogue consists in :
- when the static conditions (advance ratio, lift and propulsive force and zero first harmonic flapping conditions) are reached, the pilot initialises the excitation process. The acquisition system gives the authorisation to start the excitations to the computer for dynamic control thanks to a RS232 connection ;
- when the desired frequency and amplitude are reached, the computer for dynamic control sends an acquisition authorisation to the acquisition system (also via the RS232 channel) and the acquisition of the different sensors is performed ;
- the authorisation to change the frequency is sent from the acquisition system to the computer for dynamic control and so on, until the last required frequency.

The acquisitions were recorded at 128 points per revolution over 32 revolutions and the filters bandwidth was 0 - 200 Hz. For this kind of test a perfect transfer function determination is possible only if all the measurement channels have strictly the same characteristics. So before and after each run a check of all the filter delays was realised. The maximum authorised difference is about 5° for a frequency of 128 Hz and the maximum difference measured was 2° at 128 Hz.

FFT analysis of the dynamic results was done for all the measurements. For the sensors in fixed part, it was done up to the 64th harmonic. For the sensors located in the rotating part, before FFT analysis, the COLEMAN values were calculated. For example, concerning the pitch angles of blades 1 to 4 named pp1, pp2, pp3 and pp4, the COLEMAN values were :

c-pp0 = (pp1 + pp2 + pp3 + pp4) / 4
c-ppc=((pp1-pp3)*cosΨ+(pp2-pp4)*sinΨ)/2
c-pps=((pp1-pp3)*sinΨ-(PP2-PP4)*cosΨ)/2
c-ppi = (pp1 - pp2 + pp3 - pp4) / 4
with Ψ azimuth location of blade 1.

The COLEMAN values were also computed for the blade flapping and lead-lag and the FFT analysis was done up to the 256th harmonic.

Finally, for fixed and rotating sensors, the transfer function was computed with either the pitch angle obtained from the actuator locations or the blade root pitch angle as a reference.

4. TEST RESULTS

4.1 Configuration without wind and without blade :

These tests were performed to determine the influence of the actuator inertia. Excitations in collective pitch are particularly interesting. Figure 5 shows the XB and XA transfer functions.
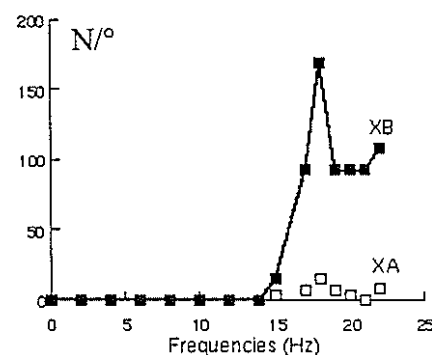

Figure 5

Above 16 Hz we enter inside the balance modes and important responses are observed on the balance (XB). But physically no effort is introduced and effectively, after inertia correction, XA results are quite equal to zero. This proves that the dynamic correction in X direction is correct (the same

comments can be made for Y direction). On another hand, figure 6 presents the transfer functions obtained in lift direction.
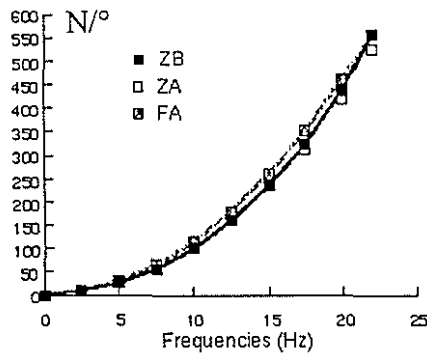

Figure 6

The level before and after inertia corrections (ZB, ZA) is nearly the same and is quite high. This phenomenon can be explained by the motion of different parts of the hub. In fact, for collective pitch excitations, the three actuators have the same vertical motion and with them the swash-plate and the pitch rods. The mass of all these parts is approximately 21.6 kg. Considering the motion of the actuators, the acceleration force FA of these different parts has been calculated. Figure 6 shows that the levels in ZA and FA are nearly the same.

4.2 Setting of frequency range

Regarding the frequency range adopted for the tests, the aim was to obtain transfer functions of the isolated rotor through a sweep which covers :

- handling qualities and low frequency dynamics phenomena felt by the pilot and/or considered as a key point for stability and control laws development,

- flap and lead-lag modes and zeros enough to identify afterwards a parametric model, which implies at least regressive and collective phenomena.

Figure 7 indicates a preliminary estimation of isolated rotor modes (Evans locus) (roots with negative imaginary part are not represented). These modes were extracted from linearization of a numeric blade element model (Eurocopter generic simulation software HOST Helicopter Overall

Simulation Tool). Blades here are considered rigid and the induced velocity model is derived from Pitt and Peters theory [2]. The dark grey area corresponds to the frequency sweep applied during most of the trials (0.5 - 14 Hz). Regarding transfer functions, they only partially cover the collective flapping mode effect on module and phase. The light grey area represents an extension to 22 Hz only tested in one case ($\mu=0.37$, $Ct/\sigma=0.075$) to allow for a complete observation of the collective flapping mode.

This particular measurements were run successfully in spite of some concern at the outset : increasing test frequency generally does not advocate for test rig safety. Moreover, coupling between flapping and induced velocity is known to increase resonance of the collective flapping mode but an accurate prediction of this effect is not easy.
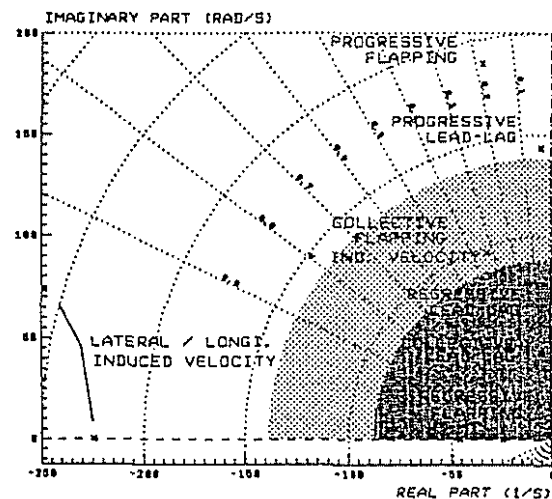

Figure 7 : frequency sweep and theoritical rotor modes

The lowest frequency is 0.5 Hz which is definitely below the slowest mode. It is however completed by a pure static measurement which consists in a stabilized response after a step input.

4.3 Validity of results

Two main kinds of input signals can be used to identify frequency responses. Either the excitation is based on a single input containing all frequencies (frequency sweep, random binary sequences, [3]), or, each frequency has to be addressed by a specific sinusoidal input.

The advantage of the first method is a shorter test duration but it offers as a counterpart an average accuracy. It is always preferred when conducting flight tests because of the first aspect. It allows saving some flight hours and also crew patience! For example, this compromise appears to be sufficient for most of the autopilot developments.

Single frequency sinusoidal inputs method obviously takes more time. As seen above, it is also more demanding regarding the quality of the signals (repeatability and synchronization of sinusoids). But, it offers the best possible accuracy.

Test duration is less critical when operating in a ground installation. Moreover, the reduced rotor model scale implies a rather high RPM (1 rev. = 16 Hz) and, consequently, faster modes. The frequency sweep can then be shifted to higher values than with a full scale rotor thus reducing inputs duration. This is why sinusoidal inputs have been chosen for these tests.

Regarding results validity, the multi-frequencies method adds to the transfer functions a special function called coherence [3]. This function is an indicator warning the user whenever some fundamental assumptions necessary to identication process are not met : noise, non-linearity, ...

In our approach, this function is not defined. Results validity is then mainly based on the observation of the fast Fourier transform (FFT) of measured signals : for each trial, the different responses are subjected to an harmonic analysis over a range $1/32 - 4 \, \Omega$ (2Ω for balance forces and moments). The intention is to check that :

- the rotor response is actually concentrated on the activated frequency which is a characteristic of linear systems,
- noise (random distribution of frequencies) remains low.

This principle is illustrated on figures 8 to 11. The examples presented here correspond to a cyclic input θ_{1S} (longitudinal command) applied with an amplitude of 1 degree.

The dominance of activated frequency on response spectrum is achieved in all cases.

The noise level is rather low (0.05 degree for flap angle, 0.02 degree for lead-lag angle). It has also been observed that this level remains rather constant whatever the input. This ensures a satisfactory identification not only for direct but also for cross-coupled responses.

As regards the lead-lag angle, the result is particularly good considering the characteristics of this point. Lead-lag modes generally present high resonances and dampers may show non-linear characteristics [4]. The selection of single frequency inputs gives an advantage because elastomeric damper responses may be degraded when using multiple frequencies excitations. Some points near lead-lag modes have been repeated several times to check the repeatability of the result.

Balance measured forces and moments at the rotor hub also show good quality results. Some noise appears on the pitching moment spectrum, but it is located beyond the objective of the measurement range and does not compromise the result. Perhaps, this indicates a balance bandwidth limitation and will have to be corrected if further experiments require a frequency sweep extension.
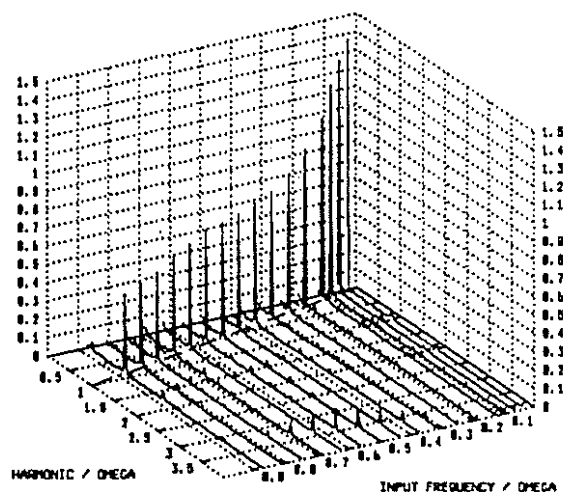

Figure 8 : harmonic analysis of β_{1C}
(input signal : θ_{1S})

The assumption of linear behaviour was also checked by changing input amplitude (1 and 0.5 degree) in some cases (near resonances). A good repeatability of transfer functions was also obtained.
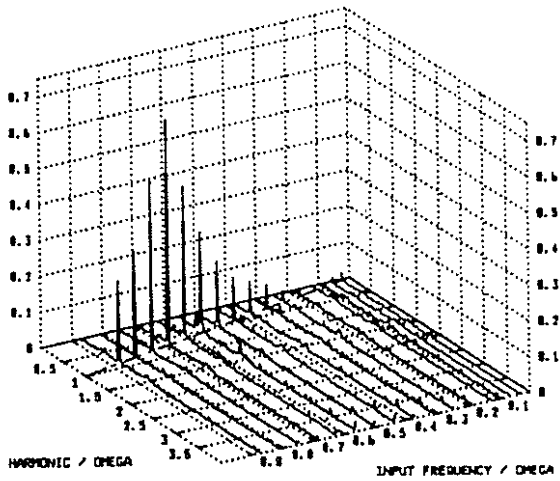
Figure 9 : harmonic analysis of δ_{1C}
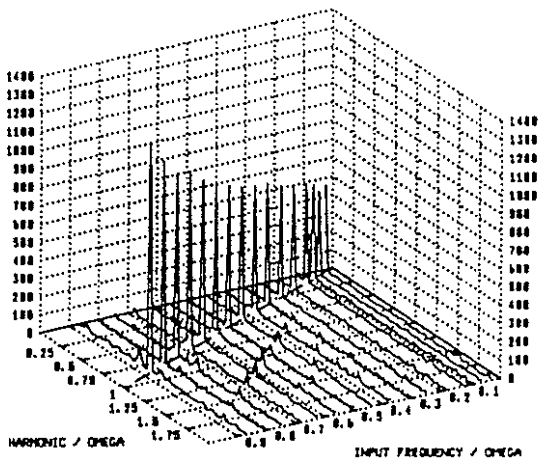(input signal : θ_{1S})

Figure 10 : harmonic analysis of vertical force
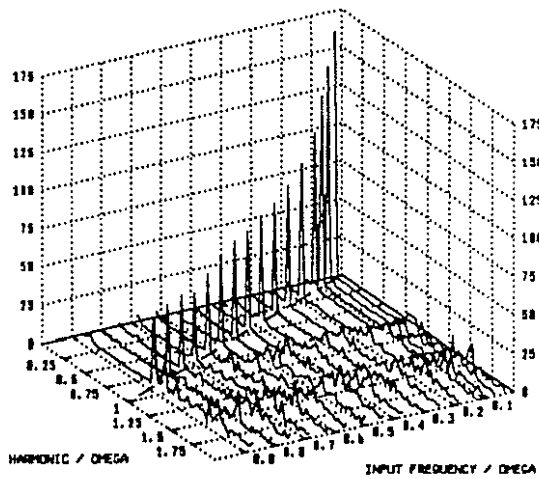(input signal : θ_{1S})

Figure 11 : harmonic analysis of pitching moment
(input signal : θ_{1S})

4.4 Transfer functions

Some results are discussed here. This first analysis is made from a simplified theory standpoint (considering rigid blades, first harmonic behaviour, ...). According to the HELIFLOW program objectives, a more detailed analysis will be undertaken in a second phase, notably through comparison with a comprehensive non-linear simulation model.

Regarding the advance ratio sweep, hover represents a reference with a minimal level of coupling between collective and cyclic phenomena and accessible to simplified theory. Its testing configuration was somewhat particular. The rotor rig was tilted 90 degrees forward in order to avoid interactions between induced velocity and the wind tunnel wall. The counterpart was the establishment of a slight flow in the wind tunnel transforming, in a way, the hover into a low vertical rate flight condition.

Figures 12 to 14 show the evolution of the flap angle responses to a collective pitch input. The coning angle static gain increases with advance ratio which is attributed both to a decrease in induced velocity and an increase in command sensitivity. Without coupling with induced velocity, the simplified theory predicts that the collective flapping mode would have a damping ratio of 0.42 (issued from Lock number characteristic). But measurements indicate a higher resonance with a damping ratio of 0.18 resulting from this coupling.
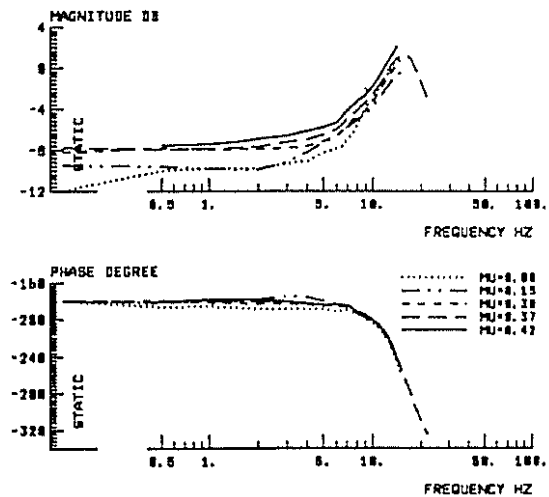

Figure 12 : transfer function β_0/θ_0

Forward flight shows a significant coupling increase on cyclic responses β_{1c}/θ_0 and β_{1s}/θ_0. In the first case, the phenomenon reminds one of command coupling (the curves reproduce the direct transfer β_{1c}/θ_{1s} with the regressive mode) whereas the second presents a different phase evolution with an increased delay that could result from axes coupling.
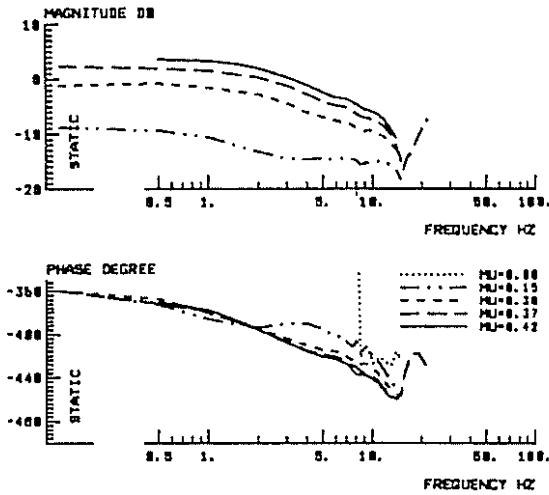

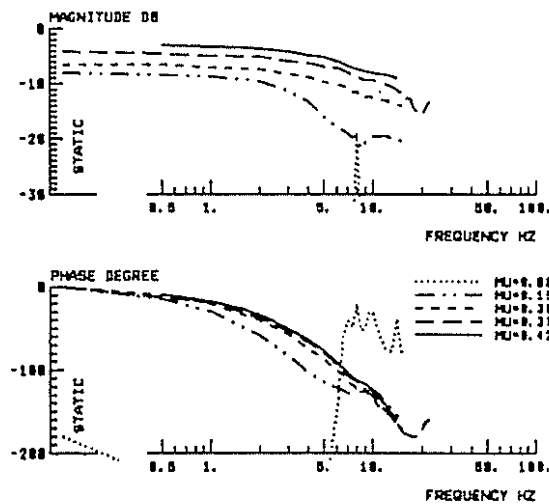Figure 13 : transfer function β_{1c}/θ_0

Figure 14 : transfer function β_{1s}/θ_0

Direct cyclic flapping responses only show moderate evolutions. Longitudinal transfer β_{1c}/θ_{1s} (figure 15) indicates a significant increase in static gain which probably comes from a change of control sensitivity. However, this goes with a bandwidth

reduction. According to the measured phase curve, the −45 degrees phase frequency (indicating regressive flap mode, [4]) goes down from 4 Hz at hover to 3 Hz at high speed. Lateral transfer β_{1s}/θ_{1c} (figure 16) does not meet such an evolution and remains rather constant when changing translation speed. This observation goes along the same lines as the simulation model including Pitt and Peters induced velocity theory [2] which predicts some modification of the regressive flap mode with speed. Coupling with induced velocity at high speed separates this second order mode into two first order modes. One of them then has a longitudinal dominant feature and presents a slightly larger time constant.
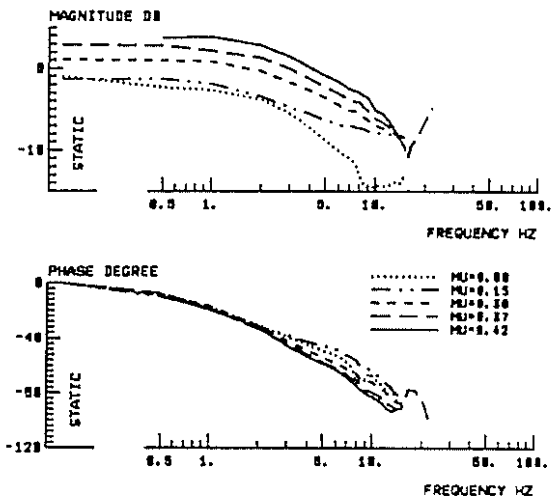

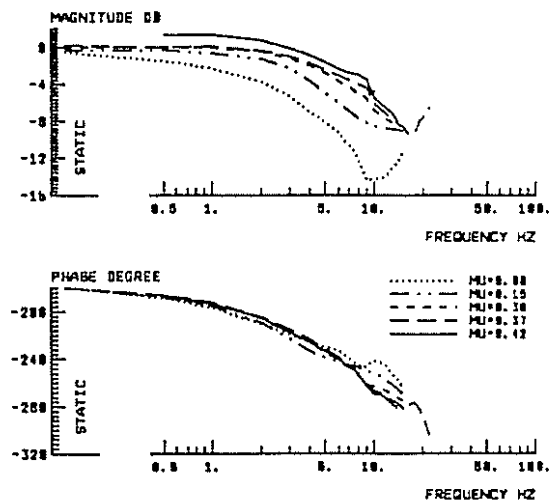Figure 15 : transfer function β_{1c}/θ_{1s}

Figure 16 : transfer function β_{1s}/θ_{1c}

Lead-lag dynamics measurements proved very good. Frequency sweep has been refined around regressive and collective modes to allow for a better observation of these low damped modes.

The low frequency gain of collective response δ_0/θ_0 (figure 17) presents a minimum for intermediate airspeed which reminds one of the static torque curve as a function of airspeed. But this time, it applies to dynamic response. According to phase curve, no change in damping appears on the collective mode.

The lead-lag regressive mode seems to lose some damping with speed. This appears on transfer functions δ_{1C}/θ_{1C} (figure 18) and δ_{1S}/θ_{1C} (not represented). Using an identification with the phase slope, the damping ratio goes down from 0.10 in hover to 0.06 at high speed (fixed frame values). Lead-lag behaviour is seldom directly affected by aerodynamics. The first interpretation that crosses one's mind is a coupling effect. This could be confirmed when looking at transfer β_{1S}/θ_{1C} (figure 16).
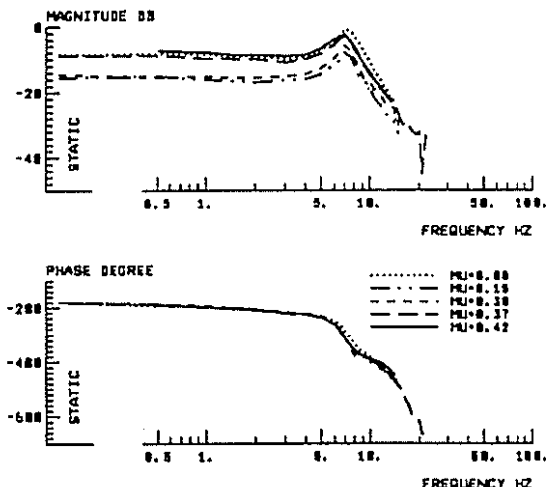

Figure 17 : transfer function δ_0/θ_0

Some slight break in slope appears on the flapping curves (both amplitude and phase) when crossing the regressive lead-lag mode frequencies (around 9 Hz) and this tendancy actually increases with airspeed.
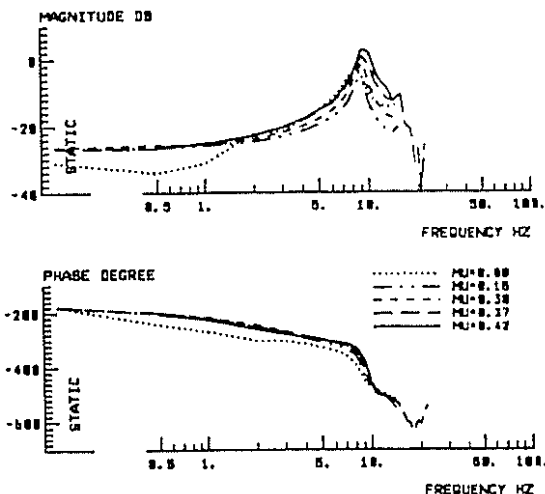

Figure 18 : transfer function δ_{1C}/θ_{1C}

The vertical force response is quite similar to coning angle transfer (β_0/θ_0, figure 12) whereas bending moments show some particularities when compared to associated flapping transfers. Static coupling of moments (figure 19) is rather high (about 30 degrees) in hover but decreases with airspeed to reach 4 degrees, contrary to flapping static coupling which remains more or less constant (about 7 degrees). In fact, simulation models generally predict lower lags between first harmonic flap angle and associated moment.

Longitudinal transfer function M_Y/θ_{1S} (figure 20) has a similar amplitude evolution with airspeed as the associated flapping response β_{1C}/θ_{1S}. On the other hand, the phase slope is not so high and strongly related to airspeed.

The observation of low frequencies moments directly addresses Handling Qualities phenomena. Most of studies devoted to improving coupling predictions by simulation are based on complete helicopter measurements and the influence of shaft motion raises some questions [5]. However, this experiment shows that a first coupling level may already appear without shaft motion.
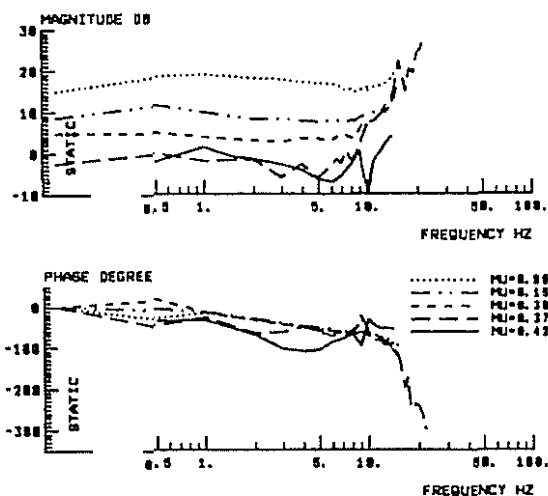
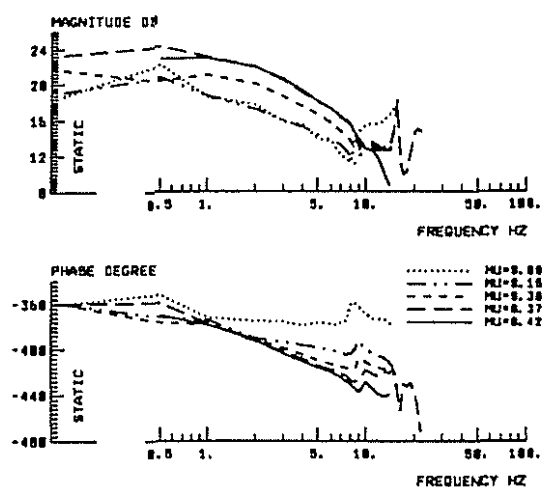**Figure 19** : transfer function M_X/θ_{1S}

Figure 20 : transfer function M_Y/θ_{1S}

5. CONCLUSION

The HELIFLOW Task 6 tests were performed in December 1997 with the ONERA rotor test rig installed in S1MA wind tunnel at Modane Avrieux Center. Single frequency sinusoidal inputs in collective, lateral and longitudinal pitch angles were realised up to 22 Hz (rotor RPM 16 Hz). The quality of the inputs is very satisfactory and the repeatability of the results is very good. Different configurations were performed covering all the level flight domain.

All this enables the determination of transfer functions of main parameters of isolated rotor with a good accuracy, especially in the case of off-axes responses. This last point is very important for simulation models validation directly addresses potential problems for flight developments.

HELIFLOW Task 6 program is still in progress and the next part plans for a more detailed analysis of measurements with comparison and improvement of simulation models.

REFERENCES

[1] M. Allongue, et al., "New Rotor Test Rig in the Large Modane Wind Tunnel", paper presented at the 15 th European Rotorcraft Forum, September 1989

[2] D.M. Pitt, D.A. Peters ''Theoritical prediction of dynamic inflow derivatives'', Vertica, vol. 15, n°1, pp. 21-34, March 1981

[3] A.M. Dequin, P. Eglin ''Validation of a flight mechanics model using frequency domain identification results on a Super Puma helicopter'', paper presented at the 20th European Rotorcraft Forum, 1994

[4] M.B. Tischler, J.T. Driscoll, M.G. Cauffman, C.J. Freedman "Study of bearingless main rotor dynamics from frequency-response wind tunnel test data", paper presented at the American Helicopter Society Aeromechanics Specialists Conference, San Francisco, CA, January 1994.

[5] M. Hossein Mansur, M.B. Tischler ''An empirical correction for improving off-axes response in flight mechanics helicopter models'', paper presented at the AGARD flight vehicle integration panel symposium on ''advances in rotorcraft technology'', May 1996